

Spectral variability of Ultra Luminous Compact X-ray Sources in Nearby Spiral Galaxies

T. Mizuno

*Department of Physics, Hiroshima University, 1-3-1 Kagamiyama, Higashi-Hiroshima, Hiroshima, Japan
739-8526*

mizuno@hirax6.hepl.hiroshima-u.ac.jp

A. Kubota and K. Makishima

Department of Physics, University of Tokyo, 7-3-1 Hongo, Bunkyo-ku, Tokyo, Japan 113-0033

ABSTRACT

Using the X-ray data taken with *ASCA*, a detailed analysis was made of intensity and spectral variations of three ultra-luminous extra-galactic compact X-ray sources (ULXs); IC 342 source 1, M81 X-6, and NGC 1313 source B, all exhibiting X-ray luminosity in the range 2×10^{39} – 1.5×10^{40} erg s⁻¹. As already reported, IC 342 source 1 showed short-term X-ray intensity variability by a factor of 2.0 on a typical time scale of 10 ks. M81 X-6 varied by a factor of 1.6 across seven observations spanning 3 years, while NGC 1313 source B varied by a factor of 2.5 between two observations conducted in 1993 July and 1995 November. The *ASCA* spectra of these sources, acquired on these occasions, were all described successfully as optically-thick emission from standard accretion disks around black holes. This confirms previous *ASCA* works which explained ULXs as mass-accreting massive black-hole binaries. In all three sources, the disk color temperature was uncomfortably high at $T_{\text{in}} = 1.0$ – 2.0 keV, and was found to vary in proportion to the square-root of the source flux. The apparent accretion-disk radius is hence inferred to change as inversely proportional to T_{in} . This suggests a significant effect of advection in the accretion disk. However, even taking this effect fully into account, the too high values of T_{in} of ULXs cannot be explained. Further invoking the rapid black-hole rotation may give a solution to this issue.

Subject headings: black hole physics — galaxies: X-rays — X-rays: galaxies

1. Introduction

One of the most puzzling aspects of X-ray emission from normal galaxies is the presence of exotic, powerful, apparently point-like X-ray sources in arm regions of some spiral galaxies (Fabbiano 1989). We call them “ultra-luminous compact X-ray sources (ULXs)”, because their luminosities, typically 10^{39} – 10^{40} erg s⁻¹, are one to two orders of magnitude higher than those of the most luminous Galactic X-ray binaries. Since the Eddington limit

for an object with mass M is expressed as

$$L_{\text{E}} = 1.5 \times 10^{38} \left(\frac{M}{M_{\odot}} \right) \text{ erg s}^{-1} \quad , \quad (1)$$

where M_{\odot} denotes the solar mass, ULXs were regarded as mass accreting black-hole binaries (BHs) involving massive (50–100 M_{\odot}) stellar-mass black holes (BHs), or neutron-star binaries (NSBs) with highly collimated X-ray emission. However, both explanations remained speculative, because X-ray spectra of ULXs were poorly known.

The breakthrough has been brought by *ASCA*

(Tanaka et al. 1994), thanks to its fine spectral capability with a modest angular resolution. Following previous works on individual ULXs (e.g., IC 342 source 1; Okada et al. 1998), Makishima et al. (2000) have performed an extensive spectral investigation of ULXs, and found that their spectra are commonly represented by a so-called multi-color disk-blackbody (MCD) model that describes emission from an accretion disk around a compact star (Mitsuda et al. 1984; Makishima et al. 1986), strongly reinforcing the BH interpretation. The MCD model provides two basic quantities of the accretion disk; the inner-most disk temperature, T_{in} , and the inner-most disk radius, R_{in} . Comparing these two quantities of ULXs with those of Galactic/Magellanic BHBs, Makishima et al. (2000) pointed out that the obtained values of T_{in} are significantly higher than those of ordinary BHBs, whereas the values of R_{in} are not so much different. Since R_{in} might correspond to the last stable orbit around a central BH, this fact implies that the mass of BHs in ULXs are relatively low ($\sim 10\text{--}20 M_{\odot}$), being inconsistent with their high luminosities. To cope with this issue, they suggested that the central BH in a ULX is rapidly rotating (i.e., a Kerr BH), hence the disk can get closer to the BH and the observed value of T_{in} can become higher. This idea was originally proposed by Zhang et al. (1997) to explain the similar high values of T_{in} found from the two Galactic jet sources, GRO J1655-40 and GRS 1915+105.

Although our understanding of ULXs have thus made a great progress, previous works have been dealing only with the time-averaged spectra, and left their spectral variability unexamined. Such a study would bring us key information on the source nature. For example, *Ginga* observations of variable Galactic/Magellanic BHBs (Ebisawa 1991; Ebisawa et al. 1993) revealed that their source luminosities vary as $\propto T_{\text{in}}^4$, or R_{in} remains constant; this fact implies that an optically-thick, geometrically-thin standard accretion disk (Shakura & Sunyaev 1973) is actually realized around a Schwarzschild BH, where the inner disk radius is defined by the last stable circular orbit. We also point out that in the ‘‘Kerr BHBs’’ scenario of ULXs, only a decrease of the inner disk radius has been considered. Needless to say, it is also necessary to examine how the relativistic effects (i.e., gravitational redshift, Doppler shifts,

and the light bending) affect the observed spectra.

Accordingly, we performed (re-)analysis of the spectra of three luminous ULXs; IC 342 source 1, M81 X-6, and NGC 1313 source B. The first has the largest flux among the observed ULXs next to M33 X-8, and showed strong short-term variability (Okada et al. 1998). The other two have relatively high fluxes and have been observed several times with *ASCA*, and are hence suitable for the study on the spectral variability. We describe the *ASCA* observation of these sources in the next section, and examine how their spectra varied in § 3. We discuss their source natures in § 4.

2. Targets and Observations

IC 342 is a nearby starburst Scd galaxy located close to the Galactic plane ($b \sim 10^\circ$). After Tully (1988), we assume the distance as 3.9 Mpc, although large optical extinction caused by the low Galactic latitude makes the distance uncertainty relatively large. This galaxy has been observed by *ASCA* twice; in 1993 September and 2000 February. As already described in Okada et al. (1998), source 1 in this galaxy exhibited a significant variability during the 1993 observation (see also Figure 1). Accordingly, we investigate the change of its spectral property in detail in § 3.1. The spectral difference between the 1993 and 2000 observations is described in a separate paper (Kubota et al. 2001).

M81 (NGC 3031) has a Cepheid-based accurate distance of 3.6 Mpc from the Hubble Space Telescope observations (Freedman et al. 1994). Fabiano (1988) observed this galaxy with *Einstein* and detected several sources, including the brightest one, called X-5 (Ishisaki et al. 1996; Iyomoto 1999) at the nucleus, and the most luminous off-nucleus source called X-6 which we study in the present paper. Due to the explosion of SN 1993J, *ASCA* has frequently observed the M81 region (Kohmura 1994; Kohmura et al. 1994; Uno 1997). Among these observations, we utilize the data obtained after 1994, in which SN 1993J had faded away significantly and its contamination to the X-6 spectrum is sufficiently low. Thus we analyzed data from seven observations in total, as shown in Table 1. Although the first two datasets were already investigated by Makishima et al. (2000), we here deal with them as well as other five, in order

to study the long-term variability. The same seven datasets were also employed by Uno (1997), in his study of SN 1993J.

NGC 1313 is a nearby face-on, late-type Sb galaxy at a distance of 4.5 Mpc (Vaucouleurs 1963). X-ray observations using *Einstein Observatory*, *ROSAT*, and *ASCA* (Fabbiano & Trinchieri 1987; Colbert et al. 1995; Miller et al. 1998; Petre et al. 1994) showed that its X-ray emission is dominated by three extremely luminous point-like sources of $L_X \sim 10^{39}$ erg s $^{-1}$ each. One of them is an X-ray luminous supernova, namely SN 1978K, and the other two are ULXs called source A and source B after Petre et al. (1994). The former is located close ($\sim 45''$) to the galaxy nucleus, whereas the latter is seen at the south-end of the host galaxy. This galaxy has been observed by *ASCA* twice, in 1993 July and in 1995 November. Makishima et al. (2000) studied source B, and showed that the spectrum of this source on either occasion can be expressed by the MCD model with different values of T_{in} . We here investigate this ULX for both observations in § 3.3, concentrating on the spectral variability. As for source A, the two observations will be compared in another paper (T. Mizuno et al. in preparation).

The observational log of our target sources is summarized in Table 1. For M81 X-6, we did not use the GIS data (see § 3.2). The GIS data for NGC 1313 in the second observation was acquired in a bit assignment (PH-X-Y-RT-SP-Time) of 8-8-8-0-0-7; this is an exceptional mode which sacrifices rise time information to improve the time resolution (in search for a pulsar in SN 1978K), so that we did not apply the off-line rise-time cut screening on the data. For the other GIS data and the SIS data, we applied a standard data screening and tabulated the net exposure in Table 1.

3. Data Analysis

3.1. IC 342 source 1

The time-averaged spectra of IC 342 source 1 were already analyzed by Okada et al. (1998) and Makishima et al. (2000). They accumulated the on-source spectra from a circular region of 3' radius on the source center, subtracted the background spectra extracted from blank-sky observations, and fitted the obtained spectra with single component models. According to their results,

the power-law model is completely unacceptable, the thermal bremsstrahlung (TBS) model provides much better value of χ^2 but is also rejected at 99% confidence level, whereas an MCD one gives an acceptable fit.

Although the short-term variability of source 1 was already sketched by Makishima (1994) and Okada et al. (1998), we reproduced its GIS light curves in Figure 1. As already reported by Makishima (1994) and Okada et al. (1998), the source exhibits clear time variability by a factor of 2 in a few hours, especially in the hard energy band. In order to study this behavior in more detail, we divided both the SIS and the GIS data into five time regions as defined in Figure 1b, and analyzed the corresponding time-sorted spectra. To grasp the rough information of the spectral variability, we first summed the phase 2 and 4 spectra into a “low-flux phase” spectra, and summed the phase 1, 3, and 5 spectra into “high-flux phase” spectra, as shown in Figure 2. In agreement with the light curves, the difference between the two spectra is more significant at higher energies, indicating that the spectrum hardens as the source flux increases. We fitted the high-flux phase SIS/GIS spectra jointly with the MCD model, and obtained the result as given in Table 2; the fit turned out to be acceptable ($\chi/\nu = 129.0/106$). We also fitted the low-flux phase spectra; the fit is again acceptable ($\chi/\nu = 115.6/107$). The best fit values of the line-of-sight absorption are $N_{\text{H}} = 4.7 \times 10^{21}$ cm $^{-2}$ for both spectra, and are consistent with the time-averaged one obtained by Makishima et al. (2000). We also found that the disk temperature differs by a factor of 1.3 between two phases, whereas the source flux by a factor of 1.7

In order to examine changes in the physical condition of the accretion disk, we calculated the values of R_{in} for the spectra of high-flux and low-flux phases. Assuming a face-on geometry, they became 112 ± 8 km and 149 ± 19 km, respectively, where we adopted the ratio of a color temperature to an effective temperature of 1.7 after Shimura & Takahara (1995), and applied a correction for the inner-disk boundary condition after Kubota et al. (1998). To our surprise, the radius R_{in} does not appear to be constant but increases as the flux decreases; this behavior contradicts that of ordinary BHBs (Ebisawa 1991; Ebisawa et al. 1993). To investigate this inference more quantitatively,

we fitted the two sets of spectra simultaneously by constraining N_{H} and R_{in} to take the same values between them (while allowing T_{in} to vary independently), and then letting R_{in} to change separately. Then, the fit improved from $\chi^2/\nu = 266.4/216$ to $\chi^2/\nu = 245.0/215$, indicating that the change of R_{in} is statistically significant (at 99% confidence level by an F -test).

Although R_{in} thus changes significantly, it might be an artifact due to wrong modeling of the spectra. For example, the MCD emission from NSBs is usually accompanied by a black-body hard component, and BHBs in the soft state often exhibit a spectral hard-tail in addition to the MCD component. Fluctuation of such a hard component, if any, might apparently cause the correlated changes of T_{in} and R_{in} seen from IC 342 source 1. We therefore tried to fit the high/low-flux phase spectra simultaneously by a common MCD model with the same R_{in} and T_{in} , adding a hard-component model to the high flux phase spectra only. The hard component was modeled by a black-body of temperature fixed at 2.0 keV, typical for NSBs (Mitsuda et al. 1984), or a power-law of photon index fixed at $\Gamma = 2.5$, nominal value for BHBs in the soft state (Tanaka & Lewin 1995). Then, the MCD plus power-law model could not explain the observed spectra ($\chi^2/\nu = 492.2/216$). The MCD plus black-body model was also statistically unacceptable ($\chi^2/\nu = 312.1/216$). Thus, the observed spectral variability cannot be due to fluctuations of the hard component, but should be attributed to the change of the MCD component itself.

We finally fitted five time-sorted spectra for the five time intervals individually by the MCD model, with the absorption fixed at the best-fit value of high/low-flux phase spectra ($N_{\text{H}} = 4.7 \times 10^{21} \text{ cm}^{-2}$). We plotted the confidence contours of the five spectra on the $T_{\text{in}}-R_{\text{in}}^2$ plane in Figure 3, where R_{in}^2 is proportional to the normalization of the MCD model. Then, like we have already found in the two phase spectral fitting, R_{in} gradually decreases as T_{in} increases, and the relation is approximately expressed as $R_{\text{in}} \propto T_{\text{in}}^{-1}$. Further examination of this result will be discussed in § 4.

3.2. M81 X-6

3.2.1. Accumulation of the source and the background spectra

When studying the spectrum of X-6, we should eliminate the contamination from the two nearby sources, SN 1993J and M81 X-5, the latter being the low-luminosity active-galactic nucleus of M81 (Ishisaki et al. 1996; Iyomoto 1999). This is because X-6 is separated only $\sim 1'$ from SN 1993J, and $\sim 3'$ from X-5, as previously reported by Kohmura et al. (1994) and Ishisaki et al. (1996).

We accumulated the source spectrum of X-6 from a circular region of $1'.5$ radius, to make the contamination from X-5 as low as possible. For the same reason, we only used the SIS data; the poorer spatial resolution of the GIS would increase the X-5 contamination. In the obtained spectrum, nevertheless, typically $\sim 50\%$ photons still originate from X-5 due to its brightness. In order to remove this residual contamination, we accumulated a background spectrum over another region having the same size as was used for the on-source spectrum. This background region is located opposite to X-6 with respect to X-5, where we expect a similar amount of contamination from X-5. We multiplied a constant factor to thus obtained background spectrum, and then subtracted it from the on-source spectrum. This ‘‘scaling factor’’ was introduced to take into account the *ASCA* XRT’s asymmetric point spread function, and was determined based on the ray-tracing (Monte-Carlo) simulation developed by the XRT team. By simulating the X-5 event for each observation (each position of X-5 on the focal plane), we can estimate the ratio of photons in the source region to the background region. The ratio, or the scaling factor, is typically 1.5, ranging over 1.2–1.8. This procedure also subtracts the non X-ray background (NXB) and the Cosmic X-ray background (CXB) after multiplying the same scaling factor, which is not precise for the NXB and CXB. However, we can neglect this effect, since the ratio of the NXB + CXB count rate to that of the contaminated photons from M81 X-5 is estimated to be $< 10\%$.

Thus, we have obtained the spectrum for X-6 plus SN 1993J. The contamination from SN 1993J is difficult to eliminate because of their short separation. Instead, we take it into account

in a different way. The SN 1993J spectrum was separately estimated by Uno (1997) through one-dimensional SIS image analysis, which was originally developed by Kohmura (1994). According to Uno (1997), SN 1993J had faded away significantly after one year from the explosion, and the spectrum is expressed by a power-law of $\Gamma = 2.5_{-0.8}^{+1.4}$ and the X-ray flux $f_X = 0.5 \pm 0.2 \times 10^{-12} \text{ erg s}^{-1} \text{ cm}^{-2}$ in 1994 April, and of $\Gamma = 3.0_{-1.0}^{+2.0}$ and $f_X = 0.2 \pm 0.1 \times 10^{-12} \text{ erg s}^{-1} \text{ cm}^{-2}$ in 1994 October, both in the 0.5–8 keV band. We calculated their contamination to the X-6 spectrum based on the ray-tracing simulation, and took the results into account as a fixed power-law component when fitting the X-6 spectrum, as indicated in Figure 4. The contribution of SN 1993J to the 0.5–10 keV flux turned out to be small; only $\sim 10\%$ and $\sim 3\%$ in 1994 April and October, respectively. For the other data which were obtained after 1995 April, we neglected the contribution from SN 1993J, since the supernova further faded away.

3.2.2. Spectra of individual observations

We fitted the obtained seven spectra separately with the typical single component models; the power-law, the TBS, and the MCD model. Then, the MCD model turned out to be always acceptable at 90% confidence level, while the TBS model provided a worse fit except for the 1995 October and 1996 October spectra (for the worst case, $\chi^2/\nu = 69.8/54$ in 1996 April). The power-law fit gave the largest values of χ^2 (1996 April data gave the worst fit of $\chi^2/\nu = 80.3/54$). Therefore we conclude that the spectra of M81 X-6, like those of IC 342 source 1, can be represented well by the single MCD model, and tabulate the MCD-fit results in Table 2. Our results for the 1994 observation are consistent with those previously reported by Makishima et al. (2000).

We plotted the obtained values of the bolometric flux of the accretion disk $f_{\text{bol}}^{\text{disk}}$ and T_{in} in Figure 5. It indicates that the seven datasets can be grossly grouped into two representative states; a low-temperature state observed in 1995 October and 1996 April, and a high-temperature state observed on the other occasions. The low/high-temperature states correspond to the low/high-flux states, so that M81 X-6 shows similar spectral variability to IC 342 source 1. We also present the

line of $f_{\text{bol}}^{\text{disk}} \propto T_{\text{in}}^4$, i.e., the locus of R_{in} remaining constant. Although the statistical errors are somewhat large, a slight deviation from this line can be inferred.

We hence made the $T_{\text{in}}-R_{\text{in}}^2$ diagram in Figure 6a, as was done on IC 342 source 1. Thus, we again, find a hint of anti-correlation between T_{in} and R_{in}^2 , like in the case of IC 342 source 1, but relatively large errors hampers definite statements. We therefore grouped the seven datasets into two spectra, i.e., the high-temperature state spectrum and the low-temperature state one. We fitted these two spectra by the same single component models as were used for each observation, and, again, the MCD model turned out to be the best representation of the data. We summarized the best fit parameters of the MCD model in Table 2, and plotted the $T_{\text{in}}-R_{\text{in}}^2$ diagram in Figure 6b, by fixing the absorption at the average value of the two states ($N_{\text{H}} = 1.8 \times 10^{21} \text{ cm}^{-2}$). Thus, R_{in} increases marginally as the flux decreases, although not so noticeable as in the case of IC 342 source 1. In fact, when we fitted the two subgrouped spectra simultaneously by constraining N_{H} and R_{in} to be common, we obtained an acceptable fit with $\chi^2/\nu=140.4/126$, while letting R_{in} to be free does not improve the fit significantly ($\chi^2/\nu=138.0/125$). Therefore R_{in} is consistent with being the same between the two spectra, although a weak anti-correlation between T_{in} and R_{in} may be present.

3.3. NGC 1313 source B

As previously reported by Makishima et al. (2000), this source showed time variability by a factor of ~ 2.5 between the 1993 and the 1995 observations. They analyzed both spectra with single component models (the power-law, the TBS, and the MCD model), and found that the MCD one gives the best description of the data. Moreover, they pointed out that the disk temperature is positively correlated with the source flux, and the value of R_{in} seemed to increase for two years whereas the source flux decreased. This behavior is therefore similar to that found with the two sources we have described so far, and we investigate the variability of this ULX in further detail.

We here utilized the same data as used by Makishima et al. (2000), and fitted them with the MCD model. We plot the confidence contours

on the $T_{\text{in}}-R_{\text{in}}^2$ plane in Figure 7, where we fixed the absorption at $N_{\text{H}} = 7 \times 10^{20} \text{ cm}^{-2}$ (the average value between the two observations). Like the two variable sources so far studied, a slight increase in R_{in} can be seen as the flux decreases. The change of R_{in} is statistically significant (at 90% confidence); we obtained an improved fit ($\chi^2/\nu=214.9/207$) when fitting the two observations simultaneously allowing R_{in} to take separate values, compared with that ($\chi^2/\nu=222.9/208$) obtained when constraining R_{in} to be common.

Since the source positions on the focal plane are largely separated ($\sim 6'$) between the two observations, the obtained value of R_{in} might be affected by the response uncertainty. According to an extensive investigation utilizing the Crab Nebula by Fukazawa et al. (1997), the calculated nominal source flux may increase artificially as the off-axis angle increases. As for our two observations, source B was observed at an off-axis angle of $\sim 10'$ and $\sim 5'$ in 1993 and 1995, respectively. Therefore, if this residual response uncertainty is present, the true 1993 flux should be lower than the estimated value. This would further enhance the increase in R_{in} for two years. We therefore conclude that the change of R_{in} seen for NGC 1313 source B is a real effect rather than an artifact.

4. Discussion

4.1. Two distinctive properties of ULXs

So far, we have been investigating the time variability of ULXs spectra, and found that they can always be represented by the MCD model, even when the source flux varies significantly. We also found that the observed flux is positively correlated with T_{in} . If R_{in} remains constant as the source flux varies like ordinary Galactic/Magellanic BHBs (Ebisawa 1991; Ebisawa et al. 1993; Kubota 2001), we will have the relation of $f_{\text{bol}}^{\text{disk}} \propto T_{\text{in}}^4$, whereas our ULXs show somewhat different relation (e.g., Figure 5). As summarized in Figure 8, they seem to obey a single common scaling of $R_{\text{in}} \propto T_{\text{in}}^{-1}$.

The observed values of T_{in} of our ULXs, ranging 1.0–2.0 keV, are also different from those of normal BHBs (typically 0.5–1.2 keV; e.g. Tanaka and Lewin 1995). Such a contradiction has been known to be a common feature of ULXs (Okada et al. 1998; Mizuno et al. 1999; Makishima et al.

2000). As previously described by Makishima et al. (2000), in the MCD approximation for the standard accretion disk around a Schwarzschild BH of mass M , T_{in} is expressed as

$$T_{\text{in}} = 1.2 \left(\frac{\xi}{0.412} \right)^{1/2} \left(\frac{\kappa}{1.7} \right) \eta^{1/4} \left(\frac{M}{10M_{\odot}} \right)^{-1/4} \text{ keV} , \quad (2)$$

where η denotes the disk bolometric luminosity normalized to the Eddington luminosity, and we have been assuming $\xi = 0.412$ and $\kappa = 1.7$. Thus, a heavier BH should show a lower value of T_{in} , as expressed by $T_{\text{in}} \propto M^{-1/4}$. Nevertheless, the ULXs that have high luminosities and hence high BH mass actually exhibit higher disk temperatures. The upper-limit on T_{in} inferred from equation 2 is 0.68 keV for the phase 1 spectra of IC342 source 1, 1.0 keV for the high-temperature phase spectra of M81 X-6, and 0.89 keV for the 1993 spectra of NGC 1313 source B even assuming a face-on geometry; these predictions contradicts the observed values by a factor of 2.9, 1.6, and 1.7, respectively. A higher disk inclination angle makes the situation even worse. Even if we exclude IC 342 source 1, for which the distance to the host galaxy is somewhat uncertain, the contradiction by a factor of $\sim \sqrt{3}$ remains to be solved.

Thus, our research with *ASCA* has provided ambivalent results on the interpretation of ULXs in terms of optically-thick standard accretion disks around massive stellar-mass BHs. On one hand, we have confirmed that the MCD model remains a good representation of the ULX spectra even when the source flux varied considerably. On the other hand, the innermost disk radius apparently changes in an anti-correlation with the disk temperature, which makes another discrepancy in addition to the previously pointed-out problem of too-high values of T_{in} (Makishima et al. 2000). In order to solve these two problems, we may introduce some modification to the standard disk picture.

4.2. Slim disk scenario

Although the standard disk model successfully explains the spectra from BHBs in the soft state, a significant progress has been achieved on the theory of accretion disks. When accretion rate \dot{M} is high and the source luminosity approaches L_{E} , the standard disk is predicted to change into a so-

called optically-thick, advection-dominated accretion flow (ADAF). This “optically-thick ADAF” model (Abramowicz et al. 1988; Szuskiwicz et al. 1996; Watarai et al. 2000) is also named a “slim accretion disk model”, since it is moderately geometrically-thick. In ULXs, because of their high luminosities, the accretion flow configuration is expected to change from the standard disk to the slim disk.

One of the most characteristic features of the slim disk, revealed by Watarai et al. (2000) through their numerical calculations, is that the X-rays are radiated not only from the regions outside the last stable orbit, but also from the regions inside it, since an abrupt change of the radial infall velocity does no longer occur. They fitted the numerically calculated slim disk spectrum by the MCD model (with R_{in} and T_{in} being the model parameters), and found that as \dot{M} increases, R_{in} decreases as $R_{\text{in}} \propto T_{\text{in}}^{-1}$. Thus, our finding of the change in R_{in} can be explained naturally by presuming that the slim disk is realized in ULXs. This suggests the presence of a slim disk in the three ULXs studied here.

Because the slim disk has a smaller R_{in} and a higher T_{in} than a standard disk in the same condition, it could also explain the “too-high T_{in} ” problem described in § 4.1. For the present three ULXs, the slim-disk scaling (the bolometric luminosity $L_{\text{bol}} \propto R_{\text{in}}^2 T_{\text{in}}^4 \propto T_{\text{in}}^2$) holds over a typical range from the observed highest luminosity L_{max} (which we tentatively identify with L_{E}) down to $\sim L_{\text{max}}/2$. While the source luminosity varies by a factor of 2, we expect the disk temperature to change by a factor of $2^{1/4}$ for the standard disk, or $2^{1/2}$ for the slim disk. In this way, the slim disk scenario can relax the too-high T_{in} problem at least by a factor of $\frac{2^{1/2}}{2^{1/4}} \sim 1.2$. However, in order to fully resolve the factor $\sqrt{3}$ discrepancy seen for our three ULXs, the source must make a transition from the standard-disk to slim-disk regimes at still lower luminosities, e.g., $L_{\text{bol}} = \frac{1}{\sqrt{3}} L_{\text{E}} \sim 0.1 L_{\text{E}}$. This contradicts the observed results of Galactic/Magellanic BHBs, where the standard accretion disk picture has been confirmed to be valid at least up to $\sim \frac{2}{3} L_{\text{E}}$ in case of GS 2000+25 and LMC X-3 (Ebisawa 1991; Ebisawa et al. 1993; Mineshige et al. 1994; Makishima et al. 2000).

Through the present study, we suggest that the

ULXs are in the slim-disk condition because of the $R_{\text{in}} \propto T_{\text{in}}^{-1}$ property, and that this partially explains the too-high values of T_{in} . However, we at the same time presume that the issue cannot be fully solved even assuming the slim disk hypothesis.

4.3. Spinning BH scenario

Before the present paper, some authors (Mizuno et al. 1999; Makishima et al. 2000) tried to explain the “too-high T_{in} ” of ULXs by assuming that the central BH is rapidly rotating; this “Kerr-BHB hypothesis” has first been proposed by Zhang et al. (1997) to explain the observed high temperatures of Galactic jet sources GRS 1915+105 and GRO J1655-40. In this subsection, we examine whether the remaining inconsistency seen for our ULXs can be solved by considering Kerr BHs or not, taking into account the relativistic effects that have not been considered by Makishima et al. (2000). Hereafter, we express the BH angular momentum J in a dimensionless manner, i.e., by a spin parameter $a^* \equiv \frac{c}{GM^2} J$. This parameter takes values between -1 to 1 ; $a_* = 1$ means the extreme Kerr hole for a prograde disk (i.e., rotating in the same direction as the BH), $a_* = -1$ also represents the extreme Kerr hole but for a retrograde disk, and $a_* = 0$ corresponds, of course, to the Schwarzschild BH.

The most immediate effect of the BH spin is that it affects the radius of the last stable orbit, R_{last} . While R_{last} is $3R_{\text{S}}$ for a Schwarzschild BH, it reduces down to $\frac{1}{2}R_{\text{S}}$ for a prograde disk around an extreme Kerr hole of $a^* = 1$ (Berdeen et al. 1972). A smaller R_{in} leads to a higher T_{in} , suggesting that the BH spin can explain the problem with ULXs.

Neglecting relativistic effects for the moment, we can perform simple quantitative estimates. For an extremely Kerr hole, R_{in} decreases by a factor of 6, or T_{in} at the luminosity maximum increases by a factor of $\sqrt{6}$. Even taking a somewhat less extreme case of $a_* = 0.95$, we expect R_{in} to decrease by a factor of 3 (or, T_{in} increases by a factor of $\sqrt{3}$) compared to the case of a Schwarzschild BH. This is apparently sufficient to explain the observed high temperatures of ULXs.

Of course, the X-ray spectra emergent from an accretion disk is subject to several relativistic cor-

rections, due to gravitational redshift, transverse and longitudinal Doppler shifts, and gravitational focusing. To a distant observer, both the observed color temperature and flux will deviate from the local values, depending on the inclination angle i . These effects have been examined through numerical calculations by several authors, including Cunningham (1975), Asaoka (1989), and Zhang et al. (1997). Employing the numerical calculation by Cunningham (1975), Zhang et al. (1997) represent the relativistic effects by two correction factors, which are to be applied on the MCD modeling of the accretion disk around a Kerr BH. One correction factor is the change of the color temperature denoted κ_{GR} , due to the gravitational redshift and Doppler red/blue-shifts. The other is the change of the flux denoted g , due to the viewing geometry and the gravitational focusing. The observed color temperature scales as $\propto \kappa_{\text{GR}}$, whereas the observed flux scales as $f_{\text{X}} \propto \frac{1}{g}$ instead of $f_{\text{X}} \propto \frac{1}{\cos^2 i}$ in the Newtonian case, where i denotes the disk inclination angle. The latter correction affects the inferred upper-limit of the disk temperature as $\propto L_{\text{bol}}^{-1/4} \propto g^{1/4}$. Further taking into account the correction due to the decrease of R_{in} , which increases the maximum disk temperature as $\propto R_{\text{in}}^{-1/2}$, we calculated the combined correction factor, $\kappa_{\text{GR}} g^{1/4} R_{\text{in}}^{-1/2}$, for a nearly-extreme Kerr holes as shown in Figure 9.

Thus, if we assume a Kerr BH of $a_* = 0.998$, and view the disk from an inclination angle of $i \geq 65^\circ$, the correction factor exceeds $\sqrt{2}$. When this is combined with another factor of ~ 1.2 due to the slim-disk property (§ 4.2), we can explain the discrepancy by a factor of $\sqrt{3}$ seen for ULXs. Since $i \sim 60^\circ$ is what is expected on average when the disks are randomly oriented, the chance probability of finding such objects is reasonably high. We thus conclude that the mystery of ULXs may be solved in terms of the slim accretion disk and the BH rotation.

Of course, there remain many aspects of the ULXs phenomena to be examined. Observationally, an optical identification of the counter-part is important; it can help us to understand how ULXs are formed, and confirm whether they are really massive, rapidly-rotating BHs. We also need to obtain spectra with much higher quality over a wider bandpass, in order to compare them with

the theoretical predictions in detail. Theoretically, numerical models of the X-ray spectrum emergent from an accretion disk around a Kerr BH, taking into account both the relativistic and advection effects, are required. Another big theoretical issue is how to make massive ($\sim 100 M_\odot$) and rapidly rotating ($a^* \geq 0.95$) stellar-mass BHs.

REFERENCES

- Abramowicz, M.A., Czerny, B., Lasota, P., Szuszkiewicz, E. 1988, ApJ, 332, 646
- Asaoka, I. 1989, PASJ, 41, 763
- Berdeen, J.M., Press, W.H., & Teukolsky, S.A. 1972, ApJ, 178, 347
- Colbert, E.J.M., Petre, R., Schlegel, E.M., Ryder, S.D. 1995, ApJ, 446, 177
- Cunningham, T. 1975, ApJ, 202, 788
- Ebisawa, K., 1991, PhD Thesis, University of Tokyo
- Ebisawa, K., Makino, F., Mitsuda, K., Belloni, T., Cowley, A., Schmidtke, P., Treves, A. 1993, ApJ, 403, 684
- Fabbiano, G. 1988, ApJ, 325, 544
- Fabbiano, G. 1989, ARA&A, 27, 87
- Fabbiano, G., Trinchieri, G. 1987, ApJ, 315, 46
- Freedman et al. 1994, ApJ, 427, 628
- Fukazawa, Y., Ishida M., & Ebisawa, K. 1997, ASCA News No.5, 3
- Ishisaki et al. 1996, PASJ, 48, 237
- Iyomoto, N. 1999, PhD Thesis, The University of Tokyo.
- Kohmura Y. 1994, PhD Thesis, The University of Tokyo
- Kohmura, Y. et al. 1994, PASJ. 46, L157
- Kubota, A., Tanaka, Y., Makishima, K., Ueda, Y., Dotani, T., Inoue, H., Yamaoka, K. 1998, PASJ, 50, 667
- Kubota, A. et al. 2001, ApJ, in press

- Kubota A. 2001, PhD Thesis, The University of Tokyo
- Miller, S., Schlegel, E.M., Petre, R., Colbert E.J.M. 1998, ApJ 116, 1657
- Makishima, K., Maejima, Y., Mitsuda, K., Brandt, H. V., Remillard, R. A., Tuohy, I. R., Hoshi, R., Nakagawa, M. 1986, ApJ, 308, 635
- Makishima, K. 1994, in *New Horizon of X-ray Astronomy*, ed F. Makino, T. Ohashi (University Academy Press, Tokyo), p171
- Makishima et al. 2000, ApJ, 535, 632
- Mineshige, S., Hirano, A., Kitamoto, S., Yamada, T. 1994, ApJ, 426, 308
- Mitsuda et al. 1984, PASJ, 36, 741
- Mizuno, T., Ohnishi, T., Kubota, A., Makishima, K., Tashiro, M. 1999 PASJ51, 663
- Okada, K., Dotani, T., Makishima, K., Mitsuda, K., Mihara, T. 1998, PASJ, 50, 25
- Petre, R., Okada, K., Mihara, T., Makishima, K., Colbert, E.J.M. 1994, PASJ, 46, L115
- Shakura, N. I., & Sunyaev, R. A. 1973, A&A, 24, 337
- Shimura, T., & Takahara, F. 1995, ApJ, 445, 780
- Szuskiewicz, E., Matthew, A., Malkan, A., Abramowicz, M. A. 1996, ApJ, 458, 474
- Tanaka, Y., Inoue, H., & Holt, S. S. 1994, PASJ, 46, L37
- Tanaka, Y., & Lewin, W.H.G 1995, in *X-ray Binaries*, eds. W.H.G. Lewin, J. van paradijis, and W.P.J. van den Heuel (Cambridge University Press, Cambridge), p126
- Throne, K. S. 1974, ApJ, 191, 507
- Tully, R. B. 1988, *Nearby Galaxies Catalogue* (Cambridge University Press, Cambridge)
- Uno, S. 1997, PhD Thesis, Gakushuin University
- Vaucouleurs, G. 1963, ApJ, 137, 720
- Watarai, K., Fukue, J., & Mineshige, S. 2000, PASJ, 52, 133
- Zhang, S.N., Cui, W., & Chen, W. 1997, ApJ, 482, L155

This 2-column preprint was prepared with the AAS L^AT_EX macros v5.0.

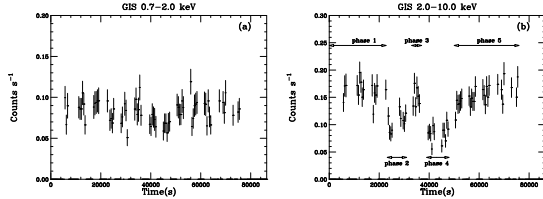


Fig. 1.— The *ASCA* GIS2 + GIS3 light curve of IC 342 source 1 including background. Panel (a) represents the light curve in the energy range of 0.7–2.0 keV, whereas panel (b) in 2.0–10 keV. The background count rate for the low and high energy range is about 0.004 c s^{-1} and 0.006 c s^{-1} , respectively.

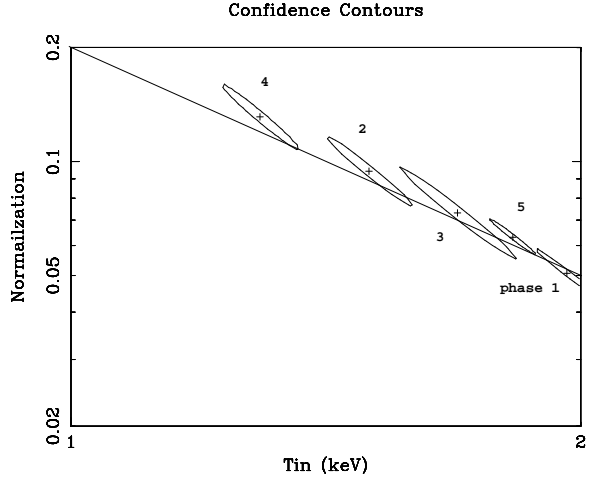


Fig. 3.— The 68% confidence contours of the short-term variations of IC342 source 1, in terms of T_{in} and the MCD normalization (proportional to R_{in}^2). The solid line represents the relation of $T_{\text{in}} \propto R_{\text{in}}^{-1}$. The horizontal axis is logarithmic.

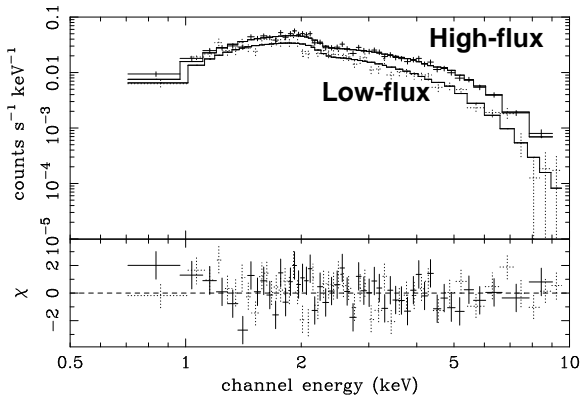


Fig. 2.— The high and the low flux phase spectra of IC 342 source 1, fitted with the MCD model. The histograms show the best fit model and the crosses represent the observed spectra. The lower panel indicates the fit residuals. Although the fit is simultaneous to the SIS and the GIS spectra, here only the GIS spectra are shown for clarity.

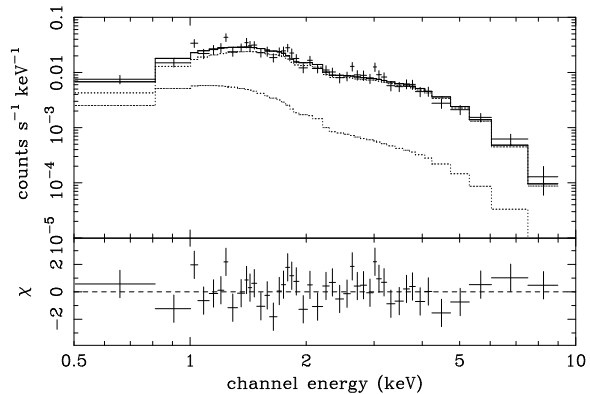


Fig. 4.— The SIS spectra of M81 X-6 obtained in 1994 April, fitted with an MCD model. Dotted lines indicate individual contributions of SN 1993J (lower one) and X-6 (higher one), with the former represented by a fixed power-law component (see text).

TABLE 1
ASCA OBSERVATIONAL LOG OF THE HOST GALAXIES.

| Galaxy | Date ^a yymmdd | Exposure (ks) ^b | | SIS Mode ^c | SIS Clock ^d |
|--------------------------------|-----------------------------|----------------------------|------|-----------------------|------------------------|
| | | SIS | GIS | | |
| IC 342 | 93 09 19 | 35.8 | 38.4 | F/B | 1111/1111 |
| NGC 3031 ^e (M81) | 94 04 01 | 31.6 | – | F/F | 1000/1000 |
| | 94 10 21 | 37.4 | – | F/F | 0010/0010 |
| | 95 04 01 | 17.6 | – | F/F | 1000/1000 |
| | 95 10 24 | 34.5 | – | F/F | 0010/0010 |
| | 96 04 16 | 43.2 | – | F/F | 1000/1000 |
| | 96 10 27 | 27.8 | – | F/F | 0010/0010 |
| | 97 05 08 | 41.0 | – | F/F | 1000/1000 |
| NGC 1313 | 93 07 12 | 21.2 | 27.7 | F/B | 1111/1111 |
| | 95 11 29 | 33.2 | 32.9 | F/F | 0100/0100 |

^a Observation start date.

^b An average of the two SIS sensors or the two GIS sensors, after the data screening is applied.

^c Data acquisition mode for Bit-High/Bit-Medium.

^d Clocking mode of S0 for Bit-High/Bit-Medium.

^e The GIS data are not utilized in the present study (see § 3.2).

TABLE 2
 TIME-RESOLVED ULX SPECTRA FITTED BY THE MCD MODEL. ERRORS ARE CALCULATED FOR 90%
 CONFIDENCE FOR ONE INTERESTING PARAMETER ($\Delta\chi^2 = 2.7$).

| Source | N_{H} (10^{22} cm^{-2}) | T_{in} (keV) | $f_{\text{bol}}^{\text{disk}\dagger}$ | χ^2/ν |
|-----------------|---|--------------------------|---------------------------------------|--------------|
| IC 342 source 1 | | | | |
| high-flux | 0.47 ± 0.04 | 1.87 ± 0.07 | 15.5 | 129.0/106 |
| low-flux | 0.47 ± 0.07 | 1.42 ± 0.09 | 8.95 | 115.6/107 |
| M81 X-6 | | | | |
| 1994 April | 0.19 ± 0.06 | 1.63 ± 0.19 | 3.61 | 43.8/42 |
| 1994 October | 0.23 ± 0.06 | 1.51 ± 0.14 | 4.05 | 34.9/47 |
| 1995 April | $0.14_{-0.11}^{+0.15}$ | 1.73 ± 0.27 | 3.71 | 29.6/23 |
| 1995 October | 0.08 ± 0.08 | $1.34_{-0.18}^{+0.23}$ | 2.48 | 17.7/21 |
| 1996 April | $0.33_{-0.14}^{+0.18}$ | $1.23_{-0.15}^{+0.18}$ | 2.78 | 61.6/54 |
| 1996 October | 0.08 ± 0.07 | $1.63_{-0.19}^{+0.23}$ | 4.14 | 30.2/31 |
| 1997 May. | 0.10 ± 0.07 | $1.61_{-0.16}^{+0.19}$ | 3.80 | 44.5/40 |
| high-temp phase | 0.16 ± 0.03 | 1.59 ± 0.09 | 3.92 | 68.6/65 |
| low-temp phase | 0.20 ± 0.08 | 1.29 ± 0.13 | 2.63 | 89.8/74 |

\dagger Bolometric flux of the accretion disk in units of $10^{-12} \text{ erg s}^{-1} \text{ cm}^{-2}$, assuming a face-on geometry.

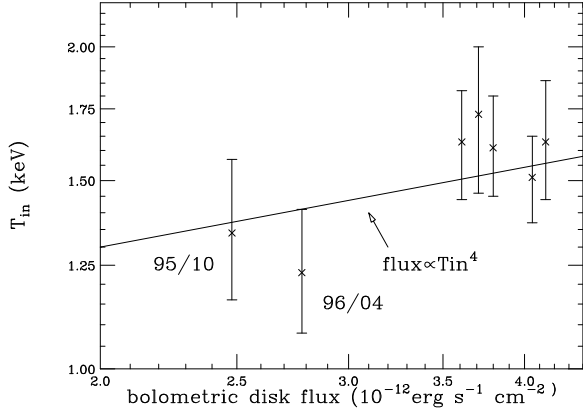


Fig. 5.— Relation between the disk bolometric flux and T_{in} for M81 X-6.

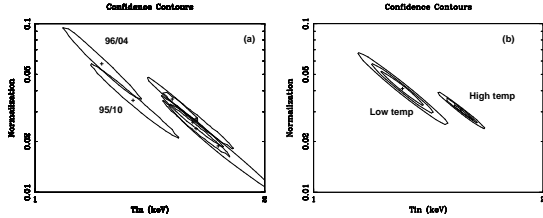


Fig. 6.— The same as Figure 3, but for M81 X-6 instead of IC 342 source 1. (a) The contours of individual observations, where only the 68% confidence levels are shown. (b) The contours of the high/low-temperature state spectra obtained by grouping the individual datasets. The 68%, 90%, and 99% confidence levels are presented.

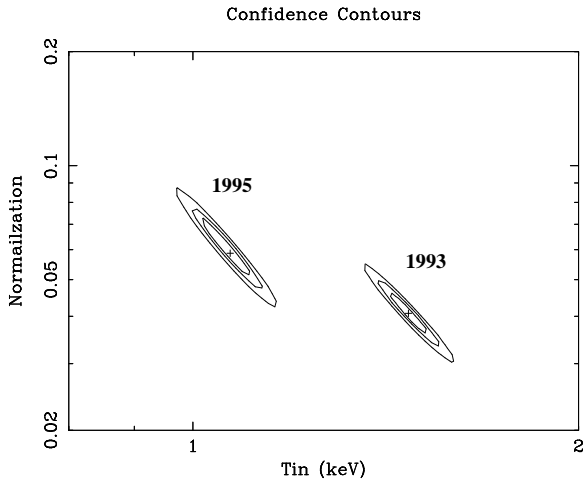


Fig. 7.— The same as Figure 3 and 6, but for the NGC 1313 source B, where 68%, 90%, and 99% confidence levels are shown.

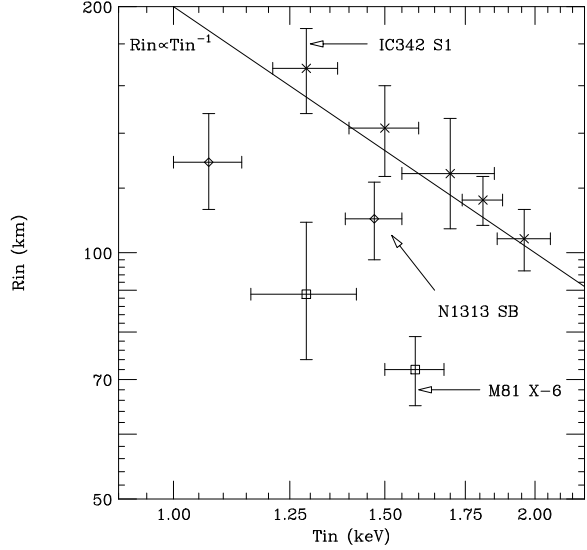


Fig. 8.— Relation between R_{in} and T_{in} for the three ULXs. The error bars represent the 90% confidence errors of the spectral fit, and the solid line indicates the relation of $R_{\text{in}} \propto T_{\text{in}}^{-1}$.

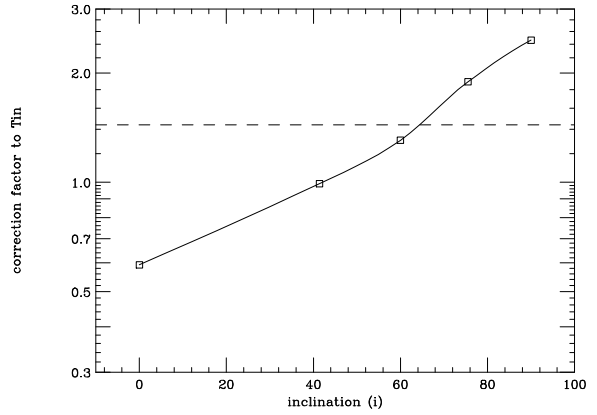


Fig. 9.— Expected increment factor of the disk temperature due to a BH rotation, relative to the Schwarzschild BH of the same mass and the same mass accretion rate. It was calculated based on the correction factor of Zhang et al (1997), for the accretion disk around a Kerr hole with $a^* = 0.9981$. This value corresponds to the case where a BH equilibrates with the disk accretion (Throne 1974). The disk is assumed to be in the regime of standard accretion disk, with no advection effects. The dashed horizontal line indicates the goal necessary to explain the high T_{in} of ULXs.